Molecular Therapy
Nucleic Acids
Original Article

ALKBH5-mediated m^{6}A mRNA methylation governs human embryonic stem cell cardiac commitment

Zhenbo Han,[1,6] Zihang Xu,[1,6] Ying Yu,[1,6] Yang Cao,[1] Zhengyi Bao,[1] Xinlu Gao,[1] Danyu Ye,[1] Gege Yan,[1] Rui Gong,[1] Juan Xu,[3] Lai Zhang,[1] Wenya Ma,[1] Xiuxiu Wang,[1] Fan Yang,[1] Hong Lei,[1] Ye Tian,[4] Shijun Hu,[5] Djibril Bamba,[1] Ying Li,[1] Desheng Li,[1] Changzhu Li,[1] Ning Wang,[1] Ying Zhang,[1] Zhenwei Pan,[1] Baofeng Yang,[1] and Benzhi Cai[1,2]

[1]Department of Pharmacy at the Second Affiliated Hospital, and Department of Pharmacology (The Key Laboratory of Cardiovascular Research, Ministry of Education) at College of Pharmacy, Harbin Medical University, Harbin 150086, China; [2]Institute of Clinical Pharmacy, the Heilongjiang Key Laboratory of Drug Research, Harbin Medical University, Harbin 150086, China; [3]Department of Bioinformatics, Harbin Medical University, Harbin 150086, China; [4]Department of Cardiology at the First Affiliated Hospital, Harbin Medical University, Harbin 150086, China; [5]Institute for Cardiovascular Science & Department of Cardiovascular Surgery of the First Affiliated Hospital, Medical College, Soochow University, Suzhou 215000, China

N6-methyladenosine (m^{6}A), as the most abundant modification of mammalian messenger RNAs, is essential for tissue development and pathogenesis. However, the biological significance of m^{6}A methylation in cardiac differentiation and development remains largely unknown. Here, we identify that the downregulation of m^{6}A demethylase ALKBH5 is responsible for the increase of m^{6}A methylation and cardiomyocyte fate determination of human embryonic stem cells (hESCs) from mesoderm cells (MESs). In contrast, ALKBH5 overexpression remarkably blocks cardiomyocyte differentiation of hESCs. Mechanistically, KDM5B and RBBP5, the components of H3K4 modifying enzyme complexes, are identified as downstream targets for ALKBH5 in cardiac-committed hESCs. Loss of function of ALKBH5 alters the expression of KDM5B and RBBP5 through impairing stability of their mRNAs, which in turn promotes the transcription of GATA4 by enhancing histone H3 Lys4 trimethylation (H3K4me3) at the promoter region of GATA4. Taken together, we reveal a previously unidentified role of m^{6}A demethylase ALKBH5 in determining cardiac lineage commitment of hESCs.

INTRODUCTION

Chemical modifications have a well-defined role in regulating the activity of mammalian messenger RNAs (mRNAs). Among over 100 types of chemical modifications,[1] N6-methyladenosine (m^{6}A) represents the most abundant form.[2–4] M^{6}A methylation is added by the m^{6}A methyltransferase complex that consists of METTL3, METTL14, and WTAP and is erased by m^{6}A demethylases ALKBH5 (α-ketoglutarate-dependent dioxygenase alkB homolog 5) and FTO (fat-mass and obesity-associated protein).[5–7] which in turn alters gene expression through controlling mRNA stability, alternative splicing, translation efficiency, and subcellular localization.[3,8–11] Recent studies have linked the dysregulation of m^{6}A methylation to cancer, obesity, and many other diseases.[10,12–16] Moreover, m^{6}A methylation is also involved in pluripotency maintenance and differentiation of embryonic stem cells (ESCs).[17–19] In particular, Bertero et al.[20] reported that SMAD2/3 could interact with the METTL3-METTL14-WTAP complex to regulate stem cell fate decisions. However, whether and how m^{6}A RNA modification regulates cardiac differentiation remains unknown.

Heart failure (HF) continues to have a high mortality rate due to the lack of effective treatments.[21] Generation of cardiomyocytes (CMs) from human pluripotent stem cells (hPSCs) has an unmet need for cell replacement therapy.[22,23] Transplantation of hPSC-derived cardiomyocytes has been shown to improve cardiac function of infarcted non-human primate heart.[24] In addition, hPSC-derived cardiomyocytes have been extensively used in drug cardiotoxicity screening, disease model establishment, and exploration of human heart development.[25,26] However, the molecular mechanism underlying cardiac differentiation remains largely unknown. Cardiogenesis of hPSCs is controlled by temporal expression of transcription factors critical for mesoderm cells (MESs) and cardiac lineage specification.[27] Recent studies have suggested that histone epigenetic modifications play a crucial role in cardiomyocyte differentiation.[28–30] Nevertheless, whether RNA m^{6}A epigenetic modification regulates cardiomyocyte differentiation is currently unknown.

Received 21 February 2020; accepted 19 May 2021;
https://doi.org/10.1016/j.omtn.2021.05.019.

[6]These authors contributed equally

Correspondence: Zhenwei Pan, Department of Pharmacy at the Second Affiliated Hospital, and Department of Pharmacology (The Key Laboratory of Cardiovascular Research, Ministry of Education) at College of Pharmacy, Harbin Medical University, Harbin 150086, China.
E-mail: panzw@ems.hrbmu.edu.cn
Correspondence: Baofeng Yang, Department of Pharmacy at the Second Affiliated Hospital, and Department of Pharmacology (The Key Laboratory of Cardiovascular Research, Ministry of Education) at College of Pharmacy, Harbin Medical University, Harbin 150086, China.
E-mail: yangbf@ems.hrbmu.edu.cn
Correspondence: Benzhi Cai, Department of Pharmacy at the Second Affiliated Hospital, and Department of Pharmacology (The Key Laboratory of Cardiovascular Research, Ministry of Education) at College of Pharmacy, Harbin Medical University, Harbin 150086, China.
E-mail: caibz@ems.hrbmu.edu.cn

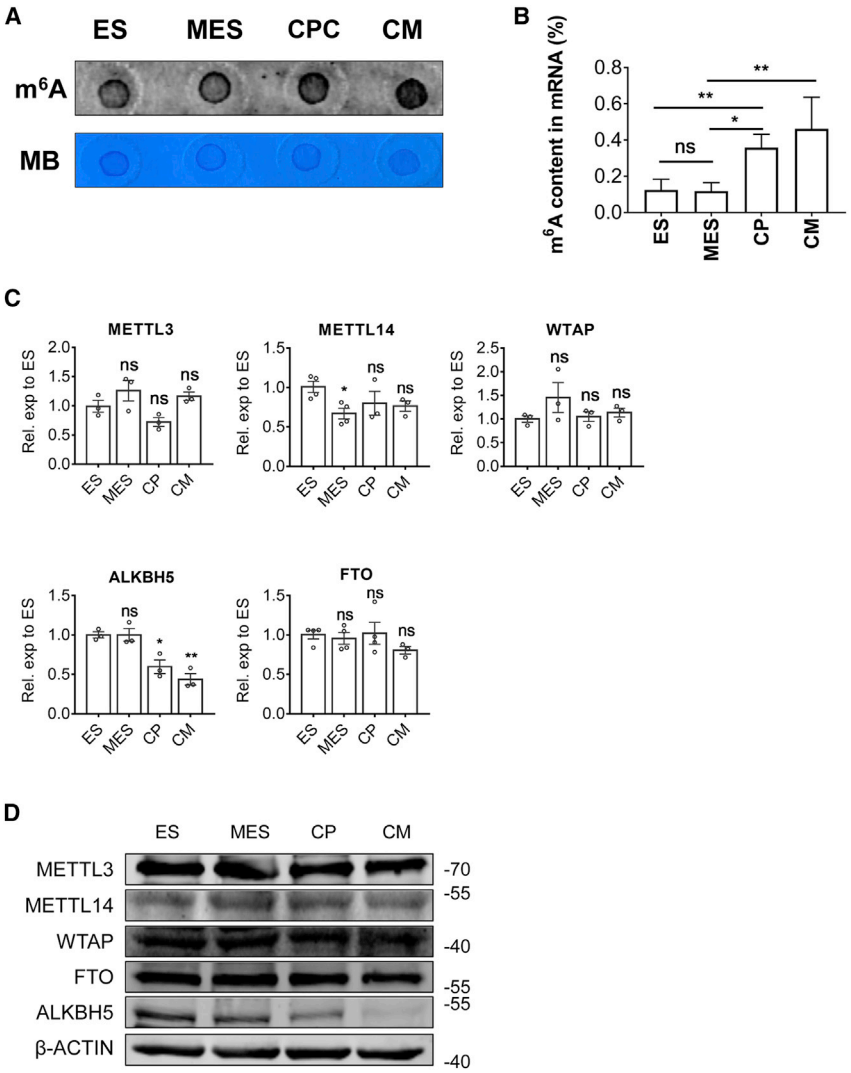

Figure 1. ALKBH5-mediated m^{6}A is induced during cardiac differentiation from mesodermal cells

(A) m^{6}A dot blot assay of hESCs, MESs, CPs, and CMs. Methylene blue staining was used as a loading control. (B) m^{6}A-ELISA assay of hESCs, MESs, CPs, and CMs. *p < 0.05 and **p < 0.01 (mean ± SEM; n = 3). (C) qRT-PCR analysis of m^{6}A modifying enzyme genes in hESCs, MESs, CPs, and CMs. *p < 0.05 and **p < 0.01 (mean ± SEM; n = 3). (D) Western blot assay of m^{6}A modifying enzyme genes in hESCs, MESs, CPs, and CMs. β-actin was used as a loading control.

RESULTS

ALKBH5-mediated m^{6}A demethylation was reduced during cardiac differentiation of mesodermal cells

To define the role of m^{6}A methylation in cardiomyocyte commitment of hESCs, we induced the differentiation of hESCs into CMs *in vitro* according to a previous report[27] (Figure S1A). Beating CMs appeared from day 7 after induction, which are highly expressed with cardiac-specific markers such as cardiac troponin T (cTnT) and α-actinin (Figures S1C and S1D). According to gene-expression patterns, the differentiation of hESCs into CMs was divided into four stages: hESCs (day 0), MESs (day 2), CPCs (cardiac progenitor cells, day 5), and CMs (day 8; Figure S1B). We performed m^{6}A dot blot analysis of mRNAs from all stages of differentiation and found that m^{6}A methylation was not affected from hESC stage to MES stage, whereas it significantly increased during the differentiation of MESs into CMs (Figure 1A). This finding was also supported by m^{6}A-ELISA assay (Figure 1B). Since the cellular level of m^{6}A methylation is determined by the activities of m^{6}A methyltransferases and demethylases, we next investigated the expression of these enzymes. We found that the expression of m^{6}A demethylase ALKBH5 was significantly decreased during the differentiation of MESs into CMs, while m^{6}A methyltransferase METTL3, METTL14, WTAP, and demethylase FTO did not alter in this stage (Figures 1C and 1D). Together, these data raise the possibility that ALKBH5-mediated m^{6}A modification may play a regulatory role in the differentiation of MESs into CMs.

Overexpression of ALKBH5 inhibited cardiac differentiation from MESs

We next examined the effect of ALKBH5-mediated m^{6}A demethylation on the lineage commitment of CMs by overexpressing this enzyme in MESs. As shown in Figures 2A–2D, transfection of ALKBH5-expressing plasmid at day 2 of differentiation dramatically elevated the RNA and protein levels of ALKBH5, which significantly decreased the global m^{6}A levels in differentiating hESCs.

In this study, we first explored the role of m^{6}A modification in cardiac differentiation and found that m^{6}A methylation was significantly upregulated upon the differentiation of MESs into CMs, which is accompanied by the decrease of m^{6}A demethylase ALKBH5. Moreover, overexpression of ALKBH5 dramatically inhibited the differentiation of MESs into CMs, indicating that m^{6}A methylation caused by the downregulation of ALKBH5 plays a critical role in cardiac differentiation. Mechanistically, m^{6}A methylation targeted mRNAs of lysine demethylase 5B (KDM5B) and retinoblastoma-binding protein 5 (RBBP5), two known H3K4me3-modifying enzymes, and regulated their activity, which in turn promoted the expression of GATA4 by enhancing histone H3 Lys4 trimethylation (H3K4me3) at its promoter region, thereby driving the cardiac differentiation of MESs. Together, our study defined the critical role of ALKBH5-mediated m^{6}A RNA modification in cardiogenesis and revealed the molecular mechanism underlying cardiac lineage commitment of human ESCs (hESCs).

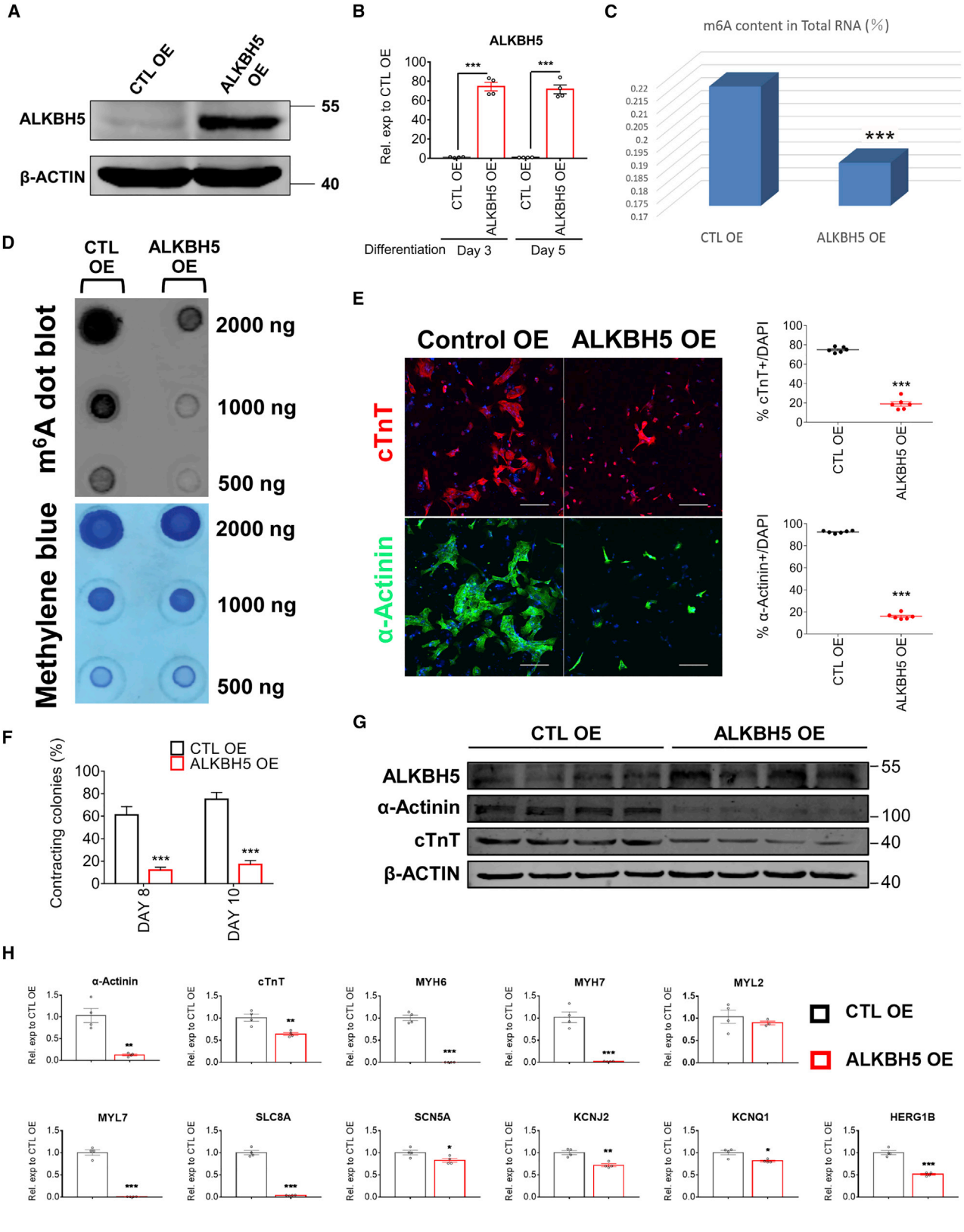

(legend on next page)

Moreover, the exogenous expression of ALKBH5 significantly reduced the percentage of $cTnT^+$ and α-$actinin^+$ cells and spontaneously contracting colonies derived from hESCs (Figures 2E and 2F). Consistent with this finding, cells expressing exogenous ALKBH5 produced much fewer cardiac genes and ion channel genes on indicated days of differentiation (Figures 2G and 2H). Together, these data suggest that ALKBH5-mediated m^6A demethylation inhibits cardiac differentiation of MESs.

Loss of ALKBH5 promoted cardiac differentiation of MESs

To further verify the role of ALKBH5 in cardiac differentiation, we inhibited its expression in MESs by using small interfering RNA (siRNA)-mediated knockdown. As shown in Figures 3A and 3B, transfections of two siRNAs targeting different regions of ALKBH5 significantly reduced both mRNA and protein levels of ALKBH5 in cells. ALKBH5 knockdown strongly elevated the level of global m^6A methylation in MESs (Figures 3C and 3D) and upregulated the expression of cardiac genes and ion channel genes in differentiated cells (Figures 3F and 3H). Moreover, MESs with less ALKBH5 had a higher propensity to generate $cTnT^+$ and α-$actinin^+$ cells and spontaneously contracting CMs (Figures 3E and 3G). Together, these data indicate that the blockage of ALKBH5-mediated m^6A demethylation promotes the differentiation of MESs into CMs.

KDM5B and RBBP5 as downstream targets of ALKBH5 that regulate the cardiac differentiation of MESs

To understand how ALKBH5-mediated m^6A demethylation regulates the cardiac commitment of MESs, we next performed m^6A transcriptomic microarray analysis to detect m^6A methylation level on which genes have changed in ALKBH5-OE differentiating hESCs compared to control. The gene ontology (GO) analysis revealed that targets of m^6A methylation were enriched in calcium signaling pathway and transcription corepression pathway (Figure 4A). Given the critical role of transcription factors such as NKX2-5, MESP1, and GATA4 in cardiac lineage specification,[30] hereby we focused on those targets that regulate transcription corepressor activity. Among them, we confirmed that the mRNA level of histone demethylase KDM5B was significantly elevated upon overexpression of ALKBH5 (Figure 4B). We next determined whether other components of histone methylation complexes were also altered by ALKBH5-mediated m^6A demethylation and found that the mRNA level of RBBP5 but not MLL1, ASH2L, and WDR5 was dramatically decreased upon ALKBH5 overexpression (Figure 4C). RBBP5 and KDM5B are two key components modulating H3K4 methylation and demethylation, respectively.[31,32] Western-blot analysis also showed that the protein level of KDM5B was significantly elevated while RBBP5 was reduced upon overexpression of ALKBH5 (Figure 4D). To the contrary, the protein expression of KDM5B was downregulated while RBBP5 was upregulated upon ALKBH5 knockdown (Figure 4E). These data imply that m^6A methylation may regulate cardiogenesis through KDM5B- and RBBP5-mediated histone modifications.

ALKBH5-mediated m^6A modification regulated H3K4me3 methylation through altering mRNA stability of KDM5B and RBBP5

To explore how ALKBH5-mediated m^6A demethylation regulates histone methylation, we carried out methylated RNA immunoprecipitation (MeRIP)-quantitative polymerase chain reaction (qPCR) assays and found that the alterations of m^6A methylation were highly enriched on mRNAs of KDM5B and RBBP5 at day 3 of differentiation (Figure 5A). Given that m^6A modification regulates gene expression mainly through altering mRNA stability, we then evaluated potential changes in RNA stability of KDM5B and RBBP5. We compared the half-lives of mRNAs of target genes with or without ALKBH5 overexpression. We found that overexpression of ALKBH5 noticeably extended the half-life of KDM5B mRNAs albeit shortened the half-life of RBBP5 mRNAs (Figure 5B). We next examined various H3 lysine methyl modifications upon ALKBH5 overexpression or knockdown. We found that the global methylation level of H3K4me3 was dramatically downregulated upon ALKBH5 overexpression and upregulated upon ALKBH5 knockdown in contrast to that of H3K9me3, H3K27me3, or H3K36me3 (Figures 5C and 5D). Immunostaining analysis also confirmed that H3K4me3 level was decreased by overexpression of ALKBH5 (Figure S2A). Together, these data suggest that ALKBH5-mediated m^6A demethylation reduced H3K4me3 methylation through altering expression of KDM5B and RBBP5.

The inhibitory role of ALKBH5 in cardiac differentiation was rescued by RBBP5 overexpression or KDM5B specific inhibitor AS8351

To confirm that RBBP5 and KDM5B are two key downstream effectors of m^6A in cardiac differentiation, we first knocked down RBBP5 by using siRNAs at day 2 of differentiation and found that it significantly decreased the methylation level of H3K4me3 (Figures 6A and 6B) and reduced the percentage of beating colonies and $cTnT^+$ and α-$actinin^+$ cells at day 10 of cardiac differentiation (Figures 6C and 6D).

On the other hand, overexpression of RBBP5 was able to promote the generation of $cTnT^+$, α-$actinin^+$, and spontaneously beating CMs,

Figure 2. Overexpression of ALKBH5 inhibits cardiac differentiation from MESs

(A) Western blot assay of ALKBH5 in control and ALKBH5 OE cells at day 3 of CM differentiation. β-actin was used as a loading control. (B) qRT-PCR analysis of ALKBH5 in control and ALKBH5 OE cells at day 3 and day 5 of CM differentiation. *$p < 0.05$, **$p < 0.01$, and ***$p < 0.005$ (mean ± SEM; n = 4). (C) m^6A-ELISA assay of control and ALKBH5 OE cells at day 3 of CM differentiation. *$p < 0.05$, **$p < 0.01$, and ***$p < 0.005$ (mean ± SEM; n = 4). (D) m^6A dot blot assay of control and ALKBH5 OE cells at day 3 of CM differentiation. Methylene blue staining was used as a loading control. (E) Immunostaining of cTnT and α-actinin in control and ALKBH5 OE cells at day 10 of CM differentiation. Scale bar, 150 μm. (F) Percentage of spontaneously contracting CMs on the days of CM differentiation following ALKBH5. *$p < 0.05$, **$p < 0.01$, and ***$p < 0.005$ (mean ± SEM). (G) Western blot assay of ALKBH5, cTnT, and α-actinin in control and ALKBH5 OE cells at day 10 of CM differentiation. β-actin was used as a loading control. (H) qRT-PCR analysis of selected genes on day 10 of CM differentiation. *$p < 0.05$, **$p < 0.01$, and ***$p < 0.005$ (mean ± SEM; n = 4).

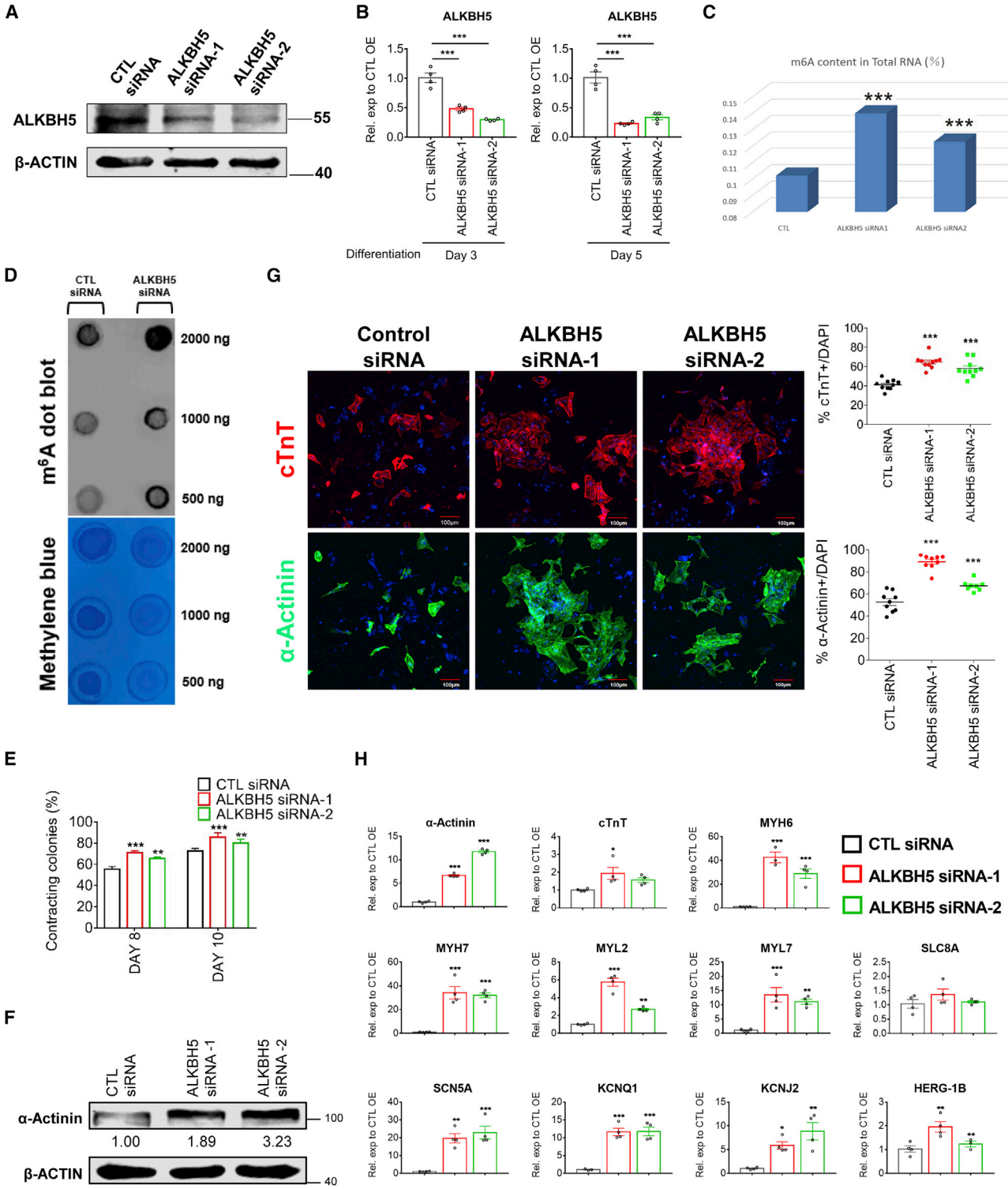

Figure 3. Lack of ALKBH5 promotes cardiac differentiation from MESs

(A) Western blot assay of ALKBH5 on day 3 in control and ALKBH5 knockdown cells. β-actin was used as a loading control. (B) qRT-PCR analysis of ALKBH5 in control and ALKBH5 KD cells at day 3 and day 5 of CM differentiation. ***$p < 0.005$ (mean ± SEM; n = 4). (C) m^6A-ELISA assay of control and ALKBH5 knockdown cells at day 3 of CM

(legend continued on next page)

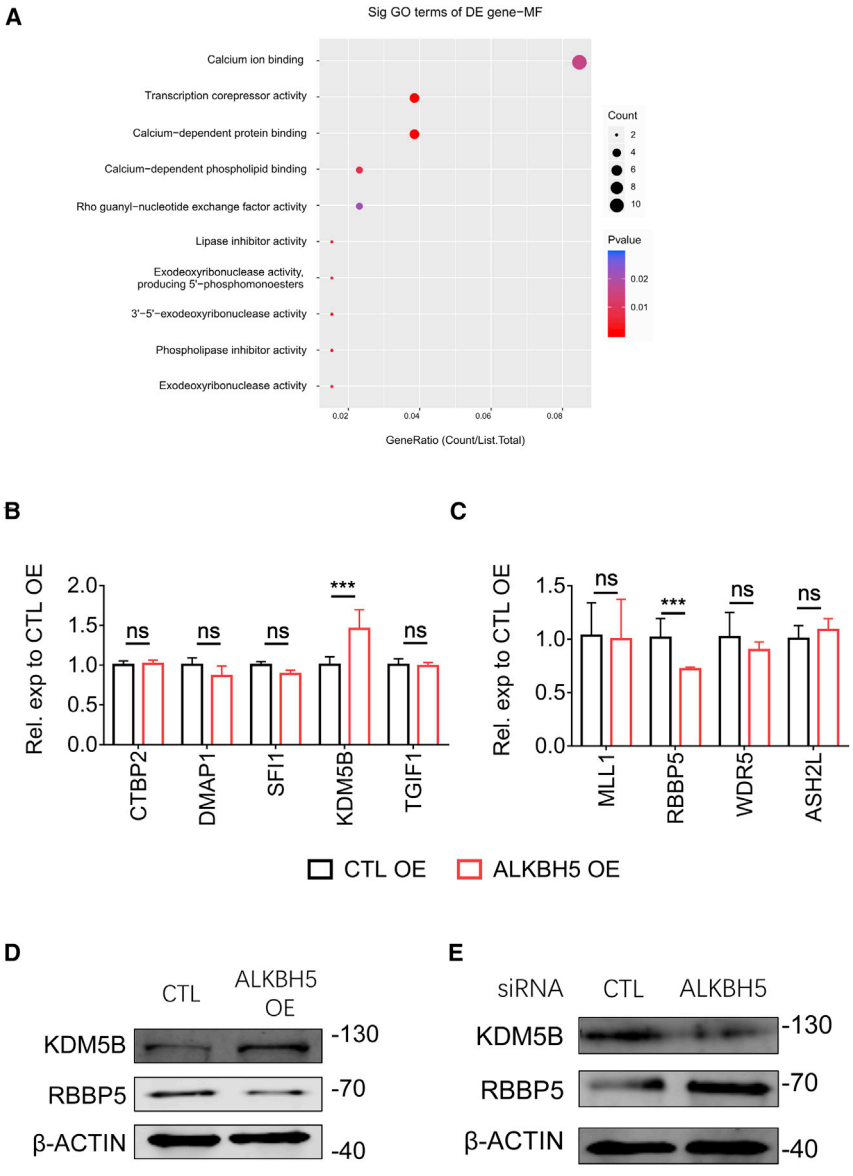

Figure 4. KDM5B and RBBP5 are potential downstream targets of ALKBH5 that regulate the cardiac differentiation of MESs

(A) GO analysis based on m^{6}A transcriptomic array. (B) qRT-PCR analysis of CTBP2, DMAP1, SFI1, KDM5B, and TGIF1 in control and ALKBH5 OE cells at day 3 of CM differentiation. *p < 0.05, **p < 0.01, and ***p < 0.005 (mean ± SEM; n = 4). (C) qRT-PCR analysis of KDM5B, MLL1, ASH2L, WDR5, and RBBP5 in control and ALKBH5 OE cells at day 3 of CM differentiation. *p < 0.05, **p < 0.01, and ***p < 0.005 (mean ± SEM; n = 4). (D) Western blot assay of RBBP5 and KDM5B on day 3 in control and ALKBH5 OE cells. β-actin was used as a loading control. (E) Western blot assay of RBBP5 and KDM5B on day 3 in control and ALKBH5 KD cells. β-actin was used as a loading control.

even with ALKBH5 overexpression (Figures 6E–6H). We then used the specific inhibitor of KDM5B, AS8351, to verify its role in m^{6}A methylation-driven cardiac differentiation and found that AS8351 treatment significantly increased global H3K4me3 methylation in differentiating hESCs (Figure 6I) and recovered the cardiac differentiation propensity of hESCs with low m^{6}A methylation, as well as the expression of cardiac genes in differentiated cells (Figure 6J; Figure S3). These results suggest that ALKBH5-mediated m^{6}A demethylation inhibits cardiac differentiation through blocking RBBP5- and KDM5B-mediated methylation of H3K4me3.

ALKBH5 decreased the H3K4me3 methylation at GATA4 promoter regions

We next addressed how m^{6}A methylation drove H3K4me3 methylation in cardiac differentiation. Cardiomyocyte lineage commitment is mainly modulated by temporal expression of transcription factors.[27] We thus checked whether KDM5B and RBBP5 were recruited to the promoter regions of these key factors and thereby regulated their expression by adding or erasing active H3K4me3 marks. We performed chromatin immunoprecipitation (ChIP)-qPCR with specific primers targeting promoter regions of key transcription factors EOMES (Eomesodermin), MESP1 (mesoderm posterior BHLH transcription factor 1), GATA4, NKX2-5 (NK2 homeobox 5), and ISL-1 (islet-1), and found that overexpression of ALKBH5 caused a noticeable downregulation of H3K4me3 methylation at the promoter region of GATA4 but not that of other factors. (Figure 7A). The co-immunoprecipitation (coIP) assays also revealed that both KDM5B and RBBP5 were associated with the GATA4 in differentiating hESCs (Figures S4A and S4B). As expected, the expression of GATA4 was dramatically decreased in cells overexpressing ALKBH5 (Figure 7B; Figure S4C). In addition, the introduction of GATA4 recovered their propensity of cardiac differentiation (Figures 7C and 7D). Altogether, these results indicate that ALKBH5-mediated

differentiation. ***p < 0.005 (mean ± SEM; n = 4). (D) m^{6}A dot blot assay of control and ALKBH5 knockdown cells at day 3 of CM differentiation. Methylene blue staining was used as a loading control. (E) Percentage of spontaneously contracting CMs on the days of CM differentiation following ALKBH5 knockdown. ***p < 0.005 (mean ± SEM). (F) Western blot assay of α-actinin in control and ALKBH5 KD cells at day 10 of CM differentiation. β-actin was used as a loading control. (G) Immunostaining of cTnT and α-actinin in control and ALKBH5 knockdown cells at day 10 of CM differentiation. Scale bar, 100 μm. (H) qRT-PCR analysis of selected genes on day 10 in control and ALKBH5 KD cells. *p < 0.05, **p < 0.01, and ***p < 0.005 (mean ± SEM; n = 4).

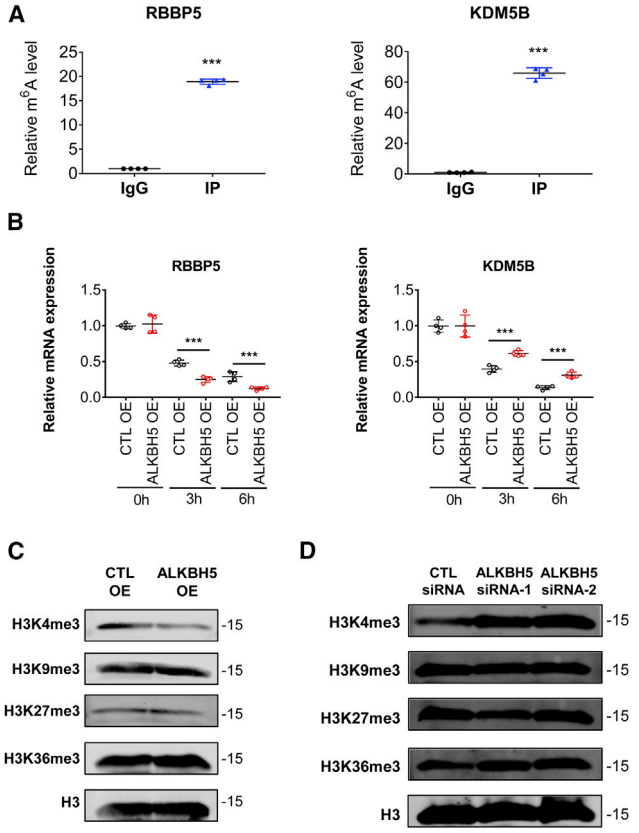

Figure 5. ALKBH5-mediated m^{6}A modification altered H3K4me3 methylation through regulates KDM5B and RBBP5 RNA stability during differentiation

(A) m^{6}A-meRIP-qPCR of RBBP5 and KDM5B in cells at day 3 of differentiation. ***$p < 0.005$ (mean ± SEM; n = 4). (B) qRT-PCR of RBBP5 and KDM5B transcripts in Act D-treated control and ALKBH5 OE differentiating cells. ***$p < 0.005$ (mean ± SEM; n = 4). (C) Western blot analysis of various H3 lysine methyl modifications in control and ALKBH5 OE cells at day 3 of CM differentiation. Total H3 was used as loading control. (D) Western blot analysis of various H3 lysine methyl modifications in control and ALKBH5 KD cells at day 3 of CM differentiation. Total H3 was used as loading control.

m^{6}A demethylation impairs the H3K4me3 methylation at GATA4 promoter regions and thereby inhibits its expression.

DISCUSSION

Recent studies have revealed that m^{6}A methylation is linked to pluripotency regulation of ESCs/induced PSCs (iPSCs). Batista et al.[18] showed that METTL3 impaired ESC exit from self-renewal toward differentiation through prolonged Nanog expression. Geula and colleagues revealed that METTL3 knockout preimplantation epiblasts and naive ESCs fail to terminate their naive pluripotent state.[33] In addition, dysregulation of m^{6}A modification could impair hematopoietic stem cell differentiation[34] and affect embryonic neural stem cell self-renewal.[35] Moreover, m^{6}A modification was also involved in spermatogonial differentiation and meiosis initiation.[36] However, the role of m^{6}A RNA modification in cardiac differentiation of stem cells remains unknown. Our study indicated that ALKBH5-mediated m^{6}A modification was significantly upregulated during the differentiation of MESs into CMs, and forced expression of ALKBH5 results in markedly inhibition of cardiac differentiation from MESs. Furthermore, ALKBH5 loss-of-function enhances the capacity of differentiation. Thus, our data demonstrate for the first time, to the best of our knowledge, that m^{6}A RNA modification plays a key role in human stem cell cardiogenesis.

Accumulating evidence has shown that epigenetic modifications play a critical role in cardiogenesis.[28–30,37,38] However, little is known regarding the contribution of histone-modifying enzymes in cardiac differentiation. Previous studies have shown that KDM5B and RBBP5 were widely associated with stem cell stemness maintenance and differentiation.[31,39,40] However, the function of KDM5B or RBBP5 in cardiac lineage commitment was unknown. Our study revealed the integral role of KDM5B and RBBP5 in cardiogenesis. coIP combined with ChIP analysis indicated that during cardiac differentiation, KDM5B and RBBP5 inhibit the transcription of GATA4 by removing active H3K4me3 marks at its promoter regions. And RBBP5 overexpression and KDM5B inhibitor AS8351 treatment ameliorated the decreased property of cardiac differentiation arising from m^{6}A reduction.

Transcription factor GATA4 is a known master regulator of cardiogenesis.[41] Our study identified ALKBH5-mediated m^{6}A modification as a regulator of GATA4 and thus uncovered the key crosstalk between m^{6}A and GATA4. This outside-in regulatory axis of ALKBH5-m^{6}A methylation-H3K4me3-GATA4 provides a novel insight into an epigenetic mechanism that controls the fate of hESC cardiac differentiation.

A recent study reported that m^{6}A methyltransferase METTL14 modulates embryonic neural stem cell self-renewal through histone H3K27 modifications.[35] Interestingly, our study indicated that m^{6}A demethylase ALKBH5 regulates hESC cardiac differentiation via H3K4 modifications. It is well documented that similar to histone modifications, DNA methylation also functions as a major epigenetic factor influencing gene activities.[42] DNA methylation is catalyzed by a family of methyltransferases (Dnmts).[43] Future studies may reveal that m^{6}A regulates DNA methylation levels via altering the expression of Dnmts.

Our findings clarify how ALKBH5-mediated m^{6}A modification regulates the differentiation of MESs into CMs. However, the functions of m^{6}A in endoderm or ectoderm differentiation still remain undefined. Further study of the roles of m^{6}A modifying enzymes in endoderm or ectoderm differentiation could largely broaden our understanding of the stem cell field. Moreover, it would be interesting to determine whether there exist different mechanisms involved in ALKBH5 induced inhibition of differentiation.

In sum, our findings demonstrate the role of ALKBH5 in hESC cardiac differentiation, highlighting the importance of m^{6}A RNA modification in heart development. These findings provide new insights into the mechanisms by which epigenetic modifications

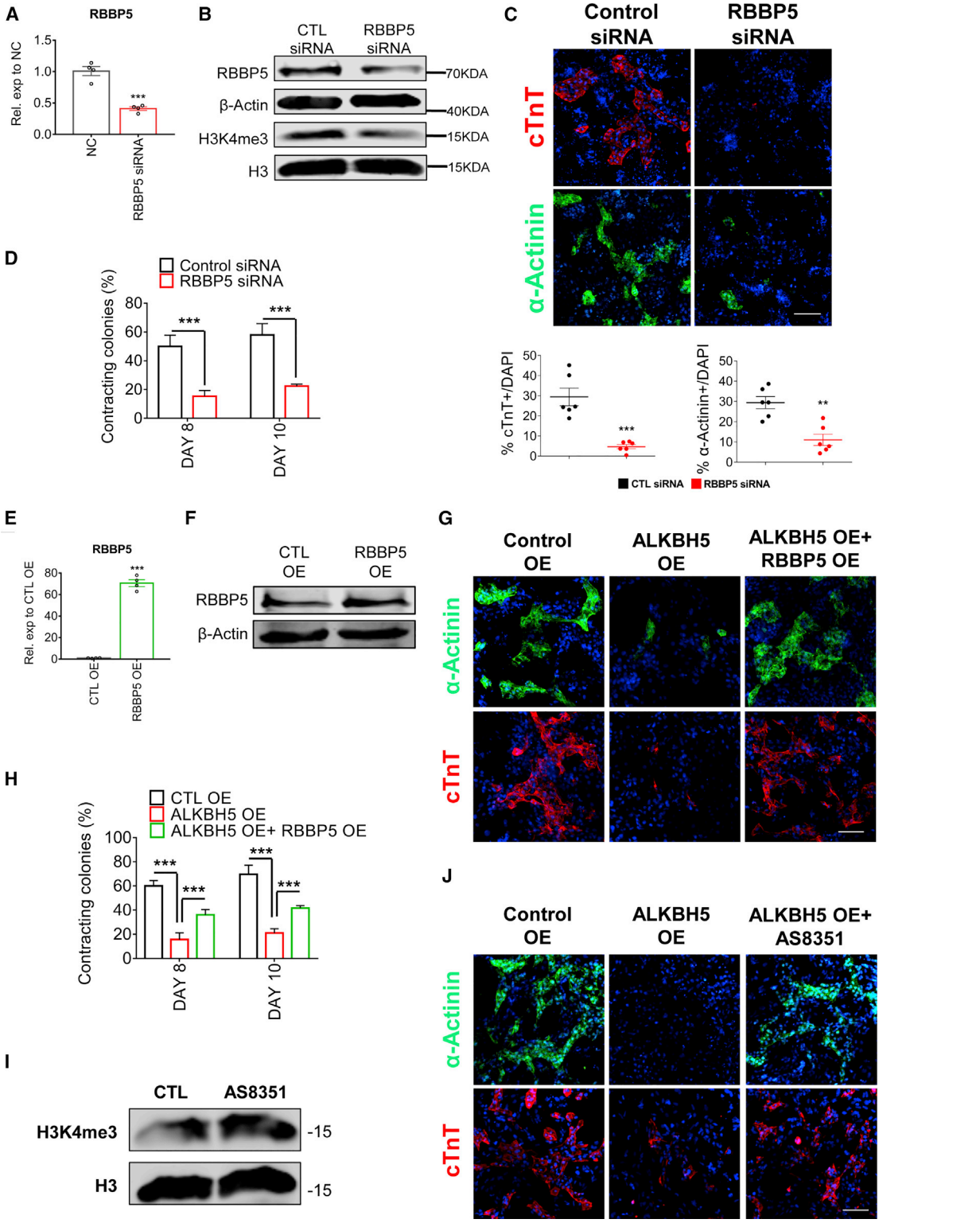

Figure 6. The inhibitory role of ALKBH5 on cardiac differentiation was rescued by RBBP5 overexpression or KDM5B-specific inhibitor AS8351

(A) qRT-PCR analysis of RBBP5 in control and RBBP5 KD cells at day 3 of CM differentiation. *p < 0.05, **p < 0.01, and ***p < 0.005 (mean ± SEM; n = 4). (B) Western blot analysis of H3K4me3 and RBBP5 in control and RBBP5 KD cells at day 3 of CM differentiation. β-actin and total H3 were used as loading controls. (C) Immunostaining of

(legend continued on next page)

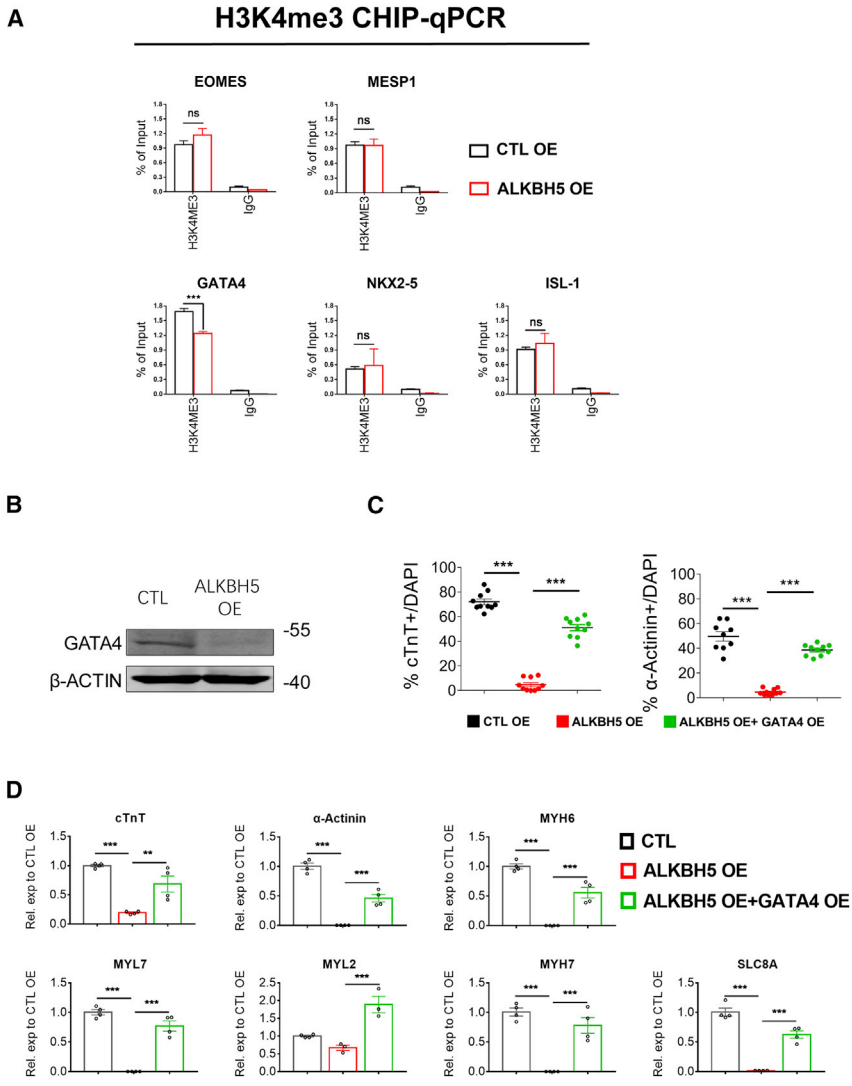

Figure 7. ALKBH5 decreases the H3K4me3 methylation at GATA4 promoter regions

(A) Enrichment of H3K4me3 at the promoters of the selected genes in ALKBH5 OE day 3 cells compared with control cells. *p < 0.05, **p < 0.01, and ***p < 0.005 (mean ± SEM; n = 4). (B) Western blot analysis of GATA4 in control and ALKBH5 OE cells at day 3 of CM differentiation. β-actin was used as a loading control. (C) Immunostaining quantification of cTnT and α-actinin in control, ALKBH5 OE, and ALKBH5 OE+GATA4 OE cells at day 10 of CM differentiation. (D) qRT-PCR analysis of selected genes on day 10 in control, ALKBH5 OE, and ALKBH5 OE+GATA4 OE cells. *p < 0.05, **p < 0.01, and ***p < 0.005 (mean ± SEM; n = 4).

regulates cardiac lineage commitment, which can be used to develop regenerative medicine solutions for congenital heart disease.

MATERIALS AND METHODS

Cell culture

hESCs were cultured as described in our previous work.[44] Cells were maintained in Essential 8 medium (05990; STEMCELL Technologies) on 1:100 basement membrane matrix-coated plates (CA3003007; Cellapy) and passaged using ethylenediaminetetraacetic acid (EDTA; Cellapy) every 3 days. Rock inhibitor Y-27632 (HY-10319, MCE) was added for 24 h after passage.

Cell transfection

We used Lipofectamine RNAiMAX for gene interference, and ViaFect Transfection Reagent was used for plasmid transfection.

The protocol of transfecting siRNA with Lipofectamine RNAiMAX Reagent is as follows: mix 6 μL of RNAiMAX in 100 μL Opti and 2 μL of siRNA in 100 μL Opti together were incubated for 5 min at room temperature in a 12-well plate when cells are 60%–80% confluent. All target sequences of siRNAs were listed in Table S4.

ViaFect Transfection Reagent was used to transfect plasmid as follows: DNA was diluted to 2 μg per 200 μL of Opti, and 8 μL ViaFect Transfection Reagent was added to achieve the proper ratio of reagent to DNA. It was incubated for 5–20 min in a 12-well plate when cells were approximately 75% confluent on the day of transfection.

Samples were collected after transfection 24 and 48 h to measure results.

Cardiomyocyte differentiation

At day 0 of cardiac differentiation, hESCs were incubated with basal medium comprising RPMI 1640 (Invitrogen) plus B27 supplement

cTnT and α-actinin in control and RBBP5 KD cells at day 10 of CM differentiation. Scale bar, 80 μm. (D) Percentage of spontaneously contracting CMs on the days of CM differentiation following knockdown of RBBP5. *p < 0.05, **p < 0.01, and ***p < 0.005 (mean ± SEM). (E) qRT-PCR analysis of RBBP5 in control and RBBP5 OE cells at day 3 of CM differentiation. *p < 0.05, **p < 0.01, and ***p < 0.005 (mean ± SEM; n = 4). (F) Western blot analysis of RBBP5 in control and RBBP5 OE cells at day 3 of CM differentiation. β-actin was used as a loading control. (G) Immunostaining of cTnT and α-actinin in control, ALKBH5 OE, and ALKBH5 OE+RBBP5 OE cells at day 10 of CM differentiation. Scale bar, 80 μm. (H) Percentage of spontaneously contracting CMs on the days of CM differentiation following ALKBH5 OE and ALKBH5 OE+RBBP5 OE. *p < 0.05, **p < 0.01, and ***p < 0.005 (mean ± SEM). (I) Western blot analysis of H3K4me3 in cells treated with 0 (control) and 1 μM AS8351. Total H3 were used as a loading control. (J) Immunostaining of cTnT and α-actinin in control, ALKBH5 OE, and ALKBH5 OE+AS8351 cells at day 10 of CM differentiation. Scale bar, 80 μm.

minus insulin (A1895601; Thermo Fisher, Waltham, MA, USA). On days 0–1, 6 μM CHIR-99021 (HY-10182; MCE, Monmouth Junction, NJ, USA) was added to the medium. On days 3–5, 2 μM wnt-C59 (HY-15659; MCE) was added to the medium. On day 7 of differentiation, the medium was changed to RPMI 1640 plus B27 supplement (17504044; Thermo Fisher). The medium was changed every 48 h. Beating cardiomyocytes appeared starting on day 7 of differentiation.

RNA extraction and quantitative real-time PCR

RNA extraction and qRT-PCR assay were performed as described in our previous studies.[45] Total RNA was isolated using miRNeasy Mini Kit (QIAGEN, 217004) according to the manufacturer's instructions and quantified by NanoDrop 8000 spectrophotometer (Gene, Shenyang, China). Then using FastStart Universal SYBR Green Master (Rox) and 7500 Fast Real-Time PCR System (Applied Biosystems, Foster City, CA, USA). Relative mRNA expression was normalized to those of housekeeping genes in each reaction. Poly(A)$^+$ mRNA were isolated by using PolyATtract mRNA Isolation Systems (Promega) in accordance with the instructions. All primer sequences are listed in Table S1.

RNA stability assay

Cells were incubated with actinomycin D (Sigma-Aldrich) at 5 μg/mL. After 0 h and 6 h of incubation, total RNA of cells was isolated for qPCR assay.

ChIP assays

ChIP assay was performed using the ChIP kit (49-2024; Invitrogen, Carlsbad, CA, USA). The methods in detail were described in our previous study.[44] The ChIP primers are listed in Table S2.

Western blotting

Cells were collected and lysed using radioimmunoprecipitation assay (RIPA) buffer (P0013; Beyotime). Protein samples were separated by sodium dodecyl sulfate-polyacrylamide gel electrophoresis and transferred to polyvinylidene fluoride (PVDF) membrane (Life Sciences, assembled in Mexico). Then membranes were washed with PBS-Tween 20 (PBST) and incubated with primary antibodies overnight at 4°C. Then cells were incubated with secondary antibodies for 1 h. Lastly, membranes were exposed to Odyssey (LI-COR Biosciences, Lincoln, NE, USA). All antibodies and their dilutions are listed in Table S3.

Co-IP

Differentiating hESCs were collected and lysed in RIPA buffer. Then 300 μg of protein was incubated with antibodies of interest conjugated with Protein A/G Magnetic Beads (HY-K0202, MCE) overnight at 4°C. The protein-bead complex was washed with IP elusion buffer (0.15 M Glycine, 0.5% Triton X-100, pH 2.5–3.1) 6 times. After discarding the supernatant, loading buffer was added and samples were heated at 100°C for 7 min for western blotting analysis.

m^{6}A-mRNA and lncRNA epitranscriptomic microarray

Total RNAs were extracted from the control group and the ALKBH5 OE group and quantified using the NanoDrop ND-1000. The RNA samples were incubated with anti-m^{6}A antibody. The m^{6}A modified RNAs were eluted from the magnetic beads as the "IP" while unmodified RNAs were recovered from the supernatant as "Sup." The "IP" and "Sup" RNAs were labeled with Cy5 and Cy3, respectively, as cRNAs using Arraystar Super RNA Labeling Kit. The cRNAs were hybridized to Arraystar Human mRNA & lncRNA Epitranscriptomic Microarray (8x60K, Arraystar). The arrays were scanned by using Agilent Scanner G2505C.

Array images were analyzed using Agilent Feature Extraction software (version 11.0.1.1). Raw intensities of "IP" and "Sup" were normalized with average of log2-scaled spike-in RNA intensities. After spike-in normalization, the probe signals having present (P) or marginal (M) QC flags in at least 1 out of 2 samples were retained as "All Targets Value" in the Excel sheet for further "m^{6}A methylation level" and "m^{6}A quantity" analyses. "m^{6}A methylation level" was calculated for the percentage of modification based on the IP (Cy5-labeled) and Sup (Cy3-labeled) normalized intensities. "m^{6}A quantity" was calculated for the m^{6}A methylation amount based on the IP (Cy5-labeled) normalized intensities. Differentially m^{6}A-methylated RNAs between two groups were identified by filtering with the fold change and statistical significance (p value) thresholds. Hierarchical clustering was performed to show the distinguishable m^{6}A-methylation pattern among samples.

MeRIP-qPCR

The level of m^{6}A modifications on genes was measured using Magna MeRIP Kit (Millipore, cat. 17-700) according to the manufacturer's instructions. Cells were harvested and lysed in lysis buffer and centrifuged at 1,500 rpm for 5 min. 5 μg m^{6}A or normal rabbit immunoglobulin G (IgG) antibody were incubated with magnetic beads and rotated for 30 min at room temperature. Beads were washed two times and then mixed with cell lysates after the lysates were thawed and centrifuged at 14,000 rpm for 10 min at 4°C. After the beads were rotated overnight at 4°C, they were washed with high salt buffer to wash off unbound materials, followed by extraction with RIP wash buffer. Each sample was analyzed by qRT-PCR.

m^{6}A dot blot assay

Cellular RNA was isolated using miRNeasy Mini Kit (QIAGEN, 217004) and quantified by NanoDrop 8000 spectrophotometer (Gene, Shenyang, China). The m^{6}A dot blot assay was performed following a previously published protocol.[46] Briefly, the RNA samples were loaded to the N$^+$ nylon membranes (RPN303B, BIOSHARP, China) then UV crosslinked using crosslinker (CL-1000, UVP). The membranes were blocked with 5% nonfat dry milk for 2 h at room temperature before they were incubated with anti-m^{6}A antibody (1:1,000 dilution, Synaptic Systems, 202003) overnight at 4°C. Then the membranes were incubated with secondary antibody for 1 h at room temperature before exposure to Odyssey (LI-COR Biosciences, Lincoln, NE, USA).

m^{6}A quantification

The quantification of m^{6}A RNA methylation level in differentiating hESCs was detected using m^{6}A RNA Methylation Quantification

Kit (Abcam, ab185912) as described by the manufacturer. Briefly, total RNA or mRNA was isolated from cells and bound to strip well for 90 min. Each well was washed and capture antibody, detection antibody, and enhancer antibody were added. Then color developing solution was added and absorbance was measured in 450 nm. Finally, to determine the relative m^{6}A RNA methylation status, the result calculation for the percentage of m^{6}A in several stages RNA was carried out using the following formula:

$$m^6A\% = \frac{(SampleOD - NCOD) \div S}{(PCOD - NCOD) \div P} \times 100\%$$

S is the amount of input sample RNA in ng.

P is the amount of input positive control in ng.

Immunofluorescence assays

Cells were fixed with 4% paraformaldehyde (PFA) before permeabilization with 0.3% Triton X-100 for 10 min. After they were blocked in goat serum, cells were then stained with primary antibodies overnight at 4°C and incubated with secondary antibodies for 1 h at room temperature. Images were captured using a live cell imaging system (Olympus Fluoview 10i). All antibodies and their dilutions are listed in Table S3.

Statistics

Error bars represent the standard error of the mean. Data were analyzed using Prism 7 (GraphPad). The significance of the differences was analyzed using one-way ANOVA and presented as *p < 0.05, **p < 0.01, and ***p < 0.005.

SUPPLEMENTAL INFORMATION

Supplemental information can be found online at https://doi.org/10.1016/j.omtn.2021.05.019.

ACKNOWLEDGMENTS

This work was supported by the National Key R&D Program of China (2017YFC1307403), the National Natural Science Fund of China (81872857/81573434/81170096/81730012/81861128022), and the Program for New Century Excellent Talents in Heilongjiang Provincial University (1252-NCET-013).

AUTHOR CONTRIBUTIONS

B.C. and Z.H. designed the project and wrote the manuscript. Z.H., Z.X. and Y.Y. performed collection and/or assembly of data, data analysis, and interpretation. Z.H., Y.Y., Z.B., X.G., D.Y., G.Y., R.G., J.X., L.Z., W.M., X.W., and F.Y., H.L., B.D., Y.L., D.L. and C.L. performed collection and/or assembly of data. Z.H., Y.T., S.H., Y.Z. and N.W. reviewed, discussed, and edited the manuscript. Z.P., B.Y., and B.C. gave final approval of manuscript and financial support.

DECLARATION OF INTERESTS

The authors declare no competing interests.

REFERENCES

1. Cantara, W.A., Crain, P.F., Rozenski, J., McCloskey, J.A., Harris, K.A., Zhang, X., Vendeix, F.A., Fabris, D., and Agris, P.F. (2011). The RNA Modification Database, RNAMDB: 2011 update. Nucleic Acids Res. *39*, D195–D201.
2. Sibbritt, T., Patel, H.R., and Preiss, T. (2013). Mapping and significance of the mRNA methylome. Wiley Interdiscip. Rev. RNA *4*, 397–422.
3. Wang, X., Lu, Z., Gomez, A., Hon, G.C., Yue, Y., Han, D., Fu, Y., Parisien, M., Dai, Q., Jia, G., et al. (2014). N6-methyladenosine-dependent regulation of messenger RNA stability. Nature *505*, 117–120.
4. Meyer, K.D., Saletore, Y., Zumbo, P., Elemento, O., Mason, C.E., and Jaffrey, S.R. (2012). Comprehensive analysis of mRNA methylation reveals enrichment in 3′ UTRs and near stop codons. Cell *149*, 1635–1646.
5. Zheng, G., Dahl, J.A., Niu, Y., Fedorcsak, P., Huang, C.M., Li, C.J., Vågbø, C.B., Shi, Y., Wang, W.L., Song, S.H., et al. (2013). ALKBH5 is a mammalian RNA demethylase that impacts RNA metabolism and mouse fertility. Mol. Cell *49*, 18–29.
6. Jia, G., Fu, Y., Zhao, X., Dai, Q., Zheng, G., Yang, Y., Yi, C., Lindahl, T., Pan, T., Yang, Y.G., and He, C. (2011). N6-methyladenosine in nuclear RNA is a major substrate of the obesity-associated FTO. Nat. Chem. Biol. *7*, 885–887.
7. Liu, J., Yue, Y., Han, D., Wang, X., Fu, Y., Zhang, L., Jia, G., Yu, M., Lu, Z., Deng, X., et al. (2014). A METTL3-METTL14 complex mediates mammalian nuclear RNA N6-adenosine methylation. Nat. Chem. Biol. *10*, 93–95.
8. Alarcón, C.R., Lee, H., Goodarzi, H., Halberg, N., and Tavazoie, S.F. (2015). N6-methyladenosine marks primary microRNAs for processing. Nature *519*, 482–485.
9. Chen, T., Hao, Y.J., Zhang, Y., Li, M.M., Wang, M., Han, W., Wu, Y., Lv, Y., Hao, J., Wang, L., et al. (2015). m(6)A RNA methylation is regulated by microRNAs and promotes reprogramming to pluripotency. Cell Stem Cell *16*, 289–301.
10. Zhao, X., Yang, Y., Sun, B.F., Shi, Y., Yang, X., Xiao, W., Hao, Y.J., Ping, X.L., Chen, Y.S., Wang, W.J., et al. (2014). FTO-dependent demethylation of N6-methyladenosine regulates mRNA splicing and is required for adipogenesis. Cell Res. *24*, 1403–1419.
11. Meyer, K.D., Patil, D.P., Zhou, J., Zinoviev, A., Skabkin, M.A., Elemento, O., Pestova, T.V., Qian, S.B., and Jaffrey, S.R. (2015). 5′ UTR m(6)A Promotes Cap-Independent Translation. Cell *163*, 999–1010.
12. Vu, L.P., Pickering, B.F., Cheng, Y., Zaccara, S., Nguyen, D., Minuesa, G., Chou, T., Chow, A., Saletore, Y., MacKay, M., et al. (2017). The N^6-methyladenosine (m^{6}A)-forming enzyme METTL3 controls myeloid differentiation of normal hematopoietic and leukemia cells. Nat. Med. *23*, 1369–1376.
13. Zhang, S., Zhao, B.S., Zhou, A., Lin, K., Zheng, S., Lu, Z., Chen, Y., Sulman, E.P., Xie, K., Bögler, O., et al. (2017). m^{6}A Demethylase ALKBH5 Maintains Tumorigenicity of Glioblastoma Stem-like Cells by Sustaining FOXM1 Expression and Cell Proliferation Program. Cancer Cell *31*, 591–606.e6.
14. Li, H.B., Tong, J., Zhu, S., Batista, P.J., Duffy, E.E., Zhao, J., Bailis, W., Cao, G., Kroehling, L., Chen, Y., et al. (2017). m^{6}A mRNA methylation controls T cell homeostasis by targeting the IL-7/STAT5/SOCS pathways. Nature *548*, 338–342.
15. Xiang, Y., Laurent, B., Hsu, C.H., Nachtergaele, S., Lu, Z., Sheng, W., Xu, C., Chen, H., Ouyang, J., Wang, S., et al. (2017). RNA m^{6}A methylation regulates the ultraviolet-induced DNA damage response. Nature *543*, 573–576.
16. Mathiyalagan, P., Adamiak, M., Mayourian, J., Sassi, Y., Liang, Y., Agarwal, N., Jha, D., Zhang, S., Kohlbrenner, E., Chepurko, E., et al. (2018). FTO-Dependent m6A Regulates Cardiac Function During Remodeling and Repair. Circulation *139*, 518–532.
17. Wen, J., Lv, R., Ma, H., Shen, H., He, C., Wang, J., Jiao, F., Liu, H., Yang, P., Tan, L., et al. (2018). Zc3h13 Regulates Nuclear RNA m^{6}A Methylation and Mouse Embryonic Stem Cell Self-Renewal. Mol. Cell *69*, 1028–1038.e6.
18. Batista, P.J., Molinie, B., Wang, J., Qu, K., Zhang, J., Li, L., Bouley, D.M., Lujan, E., Haddad, B., Daneshvar, K., et al. (2014). m(6)A RNA modification controls cell fate transition in mammalian embryonic stem cells. Cell Stem Cell *15*, 707–719.
19. Wang, Y., Li, Y., Toth, J.I., Petroski, M.D., Zhang, Z., and Zhao, J.C. (2014). N6-methyladenosine modification destabilizes developmental regulators in embryonic stem cells. Nat. Cell Biol. *16*, 191–198.
20. Bertero, A., Brown, S., Madrigal, P., Osnato, A., Ortmann, D., Yiangou, L., Kadiwala, J., Hubner, N.C., de Los Mozos, I.R., Sadée, C., et al. (2018). The SMAD2/3

interactome reveals that TGFβ controls m^{6}A mRNA methylation in pluripotency. Nature *555*, 256–259.

21. Kainuma, S., Miyagawa, S., Fukushima, S., Pearson, J., Chen, Y.C., Saito, A., Harada, A., Shiozaki, M., Iseoka, H., Watabe, T., et al. (2015). Cell-sheet therapy with omentopexy promotes arteriogenesis and improves coronary circulation physiology in failing heart. Mol. Ther *23*, 374–386.
22. Zhu, K., Wu, Q., Ni, C., Zhang, P., Zhong, Z., Wu, Y., Wang, Y., Xu, Y., Kong, M., Cheng, H., et al. (2018). Lack of Remuscularization Following Transplantation of Human Embryonic Stem Cell-Derived Cardiovascular Progenitor Cells in Infarcted Nonhuman Primates. Circ. Res. *122*, 958–969.
23. Yoshida, Y., and Yamanaka, S. (2017). Induced Pluripotent Stem Cells 10 Years Later: For Cardiac Applications. Circ. Res. *120*, 1958–1968.
24. Shiba, Y., Gomibuchi, T., Seto, T., Wada, Y., Ichimura, H., Tanaka, Y., Ogasawara, T., Okada, K., Shiba, N., Sakamoto, K., et al. (2016). Allogeneic transplantation of iPS cell-derived cardiomyocytes regenerates primate hearts. Nature *538*, 388–391.
25. Lam, C.K., and Wu, J.C. (2018). Disease modelling and drug discovery for hypertrophic cardiomyopathy using pluripotent stem cells: how far have we come? Eur. Heart J. *39*, 3893–3895.
26. Bao, Z., Han, Z., Zhang, B., Yu, Y., Xu, Z., Ma, W., Ding, F., Zhang, L., Yu, M., Liu, S., et al. (2019). Arsenic trioxide blocked proliferation and cardiomyocyte differentiation of human induced pluripotent stem cells: Implication in cardiac developmental toxicity. Toxicol. Lett. *309*, 51–58.
27. Burridge, P.W., Matsa, E., Shukla, P., Lin, Z.C., Churko, J.M., Ebert, A.D., Lan, F., Diecke, S., Huber, B., Mordwinkin, N.M., et al. (2014). Chemically defined generation of human cardiomyocytes. Nat. Methods *11*, 855–860.
28. Ohtani, K., Zhao, C., Dobreva, G., Manavski, Y., Kluge, B., Braun, T., Rieger, M.A., Zeiher, A.M., and Dimmeler, S. (2013). Jmjd3 controls mesodermal and cardiovascular differentiation of embryonic stem cells. Circ. Res. *113*, 856–862.
29. Wamstad, J.A., Alexander, J.M., Truty, R.M., Shrikumar, A., Li, F., Eilertson, K.E., Ding, H., Wylie, J.N., Pico, A.R., Capra, J.A., et al. (2012). Dynamic and coordinated epigenetic regulation of developmental transitions in the cardiac lineage. Cell *151*, 206–220.
30. Lee, J., Shao, N.Y., Paik, D.T., Wu, H., Guo, H., Termglinchan, V., Churko, J.M., Kim, Y., Kitani, T., Zhao, M.T., et al. (2018). SETD7 Drives Cardiac Lineage Commitment through Stage-Specific Transcriptional Activation. Cell Stem Cell *22*, 428–444.e5.
31. Nayak, A., Viale-Bouroncle, S., Morsczeck, C., and Muller, S. (2014). The SUMO-specific isopeptidase SENP3 regulates MLL1/MLL2 methyltransferase complexes and controls osteogenic differentiation. Mol. Cell *55*, 47–58.
32. Roesch, A., Fukunaga-Kalabis, M., Schmidt, E.C., Zabierowski, S.E., Brafford, P.A., Vultur, A., Basu, D., Gimotty, P., Vogt, T., and Herlyn, M. (2010). A temporarily distinct subpopulation of slow-cycling melanoma cells is required for continuous tumor growth. Cell *141*, 583–594.
33. Geula, S., Moshitch-Moshkovitz, S., Dominissini, D., Mansour, A.A., Kol, N., Salmon-Divon, M., Hershkovitz, V., Peer, E., Mor, N., Manor, Y.S., et al. (2015). Stem cells. m6A mRNA methylation facilitates resolution of naïve pluripotency toward differentiation. Science *347*, 1002–1006.
34. Weng, H., Huang, H., Wu, H., Qin, X., Zhao, B.S., Dong, L., Shi, H., Skibbe, J., Shen, C., Hu, C., et al. (2018). METTL14 Inhibits Hematopoietic Stem/Progenitor Differentiation and Promotes Leukemogenesis via mRNA m^{6}A Modification. Cell Stem Cell *22*, 191–205.e9.
35. Wang, Y., Li, Y., Yue, M., Wang, J., Kumar, S., Wechsler-Reya, R.J., Zhang, Z., Ogawa, Y., Kellis, M., Duester, G., and Zhao, J.C. (2018). N^6-methyladenosine RNA modification regulates embryonic neural stem cell self-renewal through histone modifications. Nat. Neurosci. *21*, 195–206.
36. Xu, K., Yang, Y., Feng, G.H., Sun, B.F., Chen, J.Q., Li, Y.F., Chen, Y.S., Zhang, X.X., Wang, C.X., Jiang, L.Y., et al. (2017). Mettl3-mediated m^{6}A regulates spermatogonial differentiation and meiosis initiation. Cell Res. *27*, 1100–1114.
37. Willems, E., and Mercola, M. (2013). Jumonji and cardiac fate. Circ. Res. *113*, 837–839.
38. Guo, X., Xu, Y., Wang, Z., Wu, Y., Chen, J., Wang, G., Lu, C., Jia, W., Xi, J., Zhu, S., et al. (2018). A Linc1405/Eomes Complex Promotes Cardiac Mesoderm Specification and Cardiogenesis. Cell Stem Cell *22*, 893–908.e6.
39. Kidder, B.L., Hu, G., and Zhao, K. (2014). KDM5B focuses H3K4 methylation near promoters and enhancers during embryonic stem cell self-renewal and differentiation. Genome Biol. *15*, R32.
40. He, R., and Kidder, B.L. (2017). H3K4 demethylase KDM5B regulates global dynamics of transcription elongation and alternative splicing in embryonic stem cells. Nucleic Acids Res. *45*, 6427–6441.
41. Ang, Y.S., Rivas, R.N., Ribeiro, A.J.S., Srivas, R., Rivera, J., Stone, N.R., Pratt, K., Mohamed, T.M.A., Fu, J.D., Spencer, C.I., et al. (2016). Disease Model of GATA4 Mutation Reveals Transcription Factor Cooperativity in Human Cardiogenesis. Cell *167*, 1734–1749, e1722.
42. Harris, C.J., Scheibe, M., Wongpalee, S.P., Liu, W., Cornett, E.M., Vaughan, R.M., Li, X., Chen, W., Xue, Y., Zhong, Z., et al. (2018). A DNA methylation reader complex that enhances gene transcription. Science *362*, 1182–1186.
43. Moore, L.D., Le, T., and Fan, G. (2013). DNA methylation and its basic function. Neuropsychopharmacology *38*, 23–38.
44. Han, Z., Yu, Y., Xu, J., Bao, Z., Xu, Z., Hu, J., Yu, M., Bamba, D., Ma, W., Ding, F., et al. (2018). Iron Homeostasis Determines Fate of Human Pluripotent Stem Cells Via Glycerophospholipids-Epigenetic Circuit. Stem Cells *37*, 489–503.
45. Han, Z., Wang, X., Xu, Z., Cao, Y., Gong, R., Yu, Y., Yu, Y., Guo, X., Liu, S., Yu, M., et al. (2021). ALKBH5 regulates cardiomyocyte proliferation and heart regeneration by demethylating the mRNA of YTHDF1. Theranostics *11*, 3000–3016.
46. Huang, H., Weng, H., Sun, W., Qin, X., Shi, H., Wu, H., Zhao, B.S., Mesquita, A., Liu, C., Yuan, C.L., et al. (2018). Recognition of RNA N^6-methyladenosine by IGF2BP proteins enhances mRNA stability and translation. Nat. Cell Biol. *20*, 285–295.